Materials Letters xx (xxxx) xxxx–xxxx

Contents lists available at ScienceDirect

Materials Letters

journal homepage: www.elsevier.com/locate/matlet

Li ion diffusion dynamics on Li oxides and peroxides surfaces

H.W. Wang[a], Z.F. Tian[a], C.Y. Ouyang[a,b,*]

[a] College of Chemical Engineering, Huanggang Normal University, Huanggang 438000, China
[b] Laboratory of Computational Materials Physics, Department of Physics, Jiangxi Normal University, Nanchang 330022, China

ARTICLE INFO

Keywords:
Energy storage and conversion
Diffusion
Surfaces, Li-O_2 batteries
Discharge product

ABSTRACT

Li ion diffusion in the discharge products of the Li-O_2 batteries is relevant to the performance of the battery. In this paper, Li ad-atom and Li-vacancy diffusion at the Li_2O and Li_2O_2 surfaces are studied from first principles calculations. Li diffusion are considered on the energetically most favorable surfaces Li_2O-(111) and Li_2O_2 ($11\bar{2}0$), which are obtained from calculating the surface energies of low index surfaces. Results show that Li diffusion on the Li_2O-(111) is very slow at room temperature with energy barriers of 0.45 eV and 0.98 eV for Li ad-atom migration and vacancy migration, respectively. On the other hand, Li diffusion on Li_2O_2 ($11\bar{2}0$) surface is even more difficult. Li-vacancy migration energy barrier is 0.75 eV, while Li ad-atom migration is prohibited with an energy barrier of 1.87 eV. These results give explanations to the poor rate performance of the Li-O_2 batteries and also suggest a possible Li_2O phase formation mechanism at the Li_2O_2 surface.

1. Introduction

Development of the electric vehicles (EVs) is restricted by the power supply technology [1]. Li-air (O_2) battery is one promising power supply for the EVs due to its high theoretical energy density [2–4]. During the discharge of a Li-air battery, the following reactions may occur at different conditions [5,6]:

$$Li+O_2 \rightarrow LiO_2$$

$$2LiO_2 \rightarrow Li_2O_2+O_2$$

$$2Li+Li_2O_2 \rightarrow 2Li_2O$$

These reactions show that LiO_2, Li_2O_2 and Li_2O are the main discharge products. It is reported that recharge of the battery is very difficult when the discharge product is Li_2O, because decomposition of the Li_2O product is very difficult and thus harmful to the reversibility of the battery [4].

The above reactions are related with the discharge potential. It is shown that the main discharge product is Li_2O when the discharge potential is lower than 2.0 V [7]. The above reactions are also strictly associated with the Li ion and O_2 mobility. One challenge of the Li-O_2 battery is to decrease the overpotential of the battery system, which is mainly caused by the slow charge carrier transportation during the charge/discharge process. The charge carrier transportation includes both electronic conduction and Li ionic diffusion, which also determine the rate performance of the battery system. Recently, it is found that the rate performance of the Li-O_2 battery is sensitive to the oxygen pressure, and the reversible capacity increases with the increased oxygen pressure [8].

During the discharge process, Li ion moves from the anode to the cathode side and adsorbed on the surface of the cathode material. When the discharge products are accumulated on the cathode surfaces, Li adsorption occurs on the surfaces of the discharged products. As a result, Li diffusion at the discharge product surface is one important issue that has strong correlation to the discharge reaction, the overpotential, and the rate capability of the Li-O_2 battery.

In this paper, using first principles calculations, we studied the Li ion diffusion on the stable surfaces of two main discharge products, namely, Li_2O-(111) and Li_2O_2 ($11\bar{2}0$) surfaces. The results are helpful to the understanding of the operation of the Li-O_2 battery, and thus beneficial to design the Li-O_2 battery system.

2. Computational details

Computations are performed using the Vienna *ab initio* simulation package (VASP) [9] based on the density functional theory (DFT) and pseudopotential method. The core ion and valence electron interaction is described by the projector augmented wave method (PAW) [10] and the electron exchange-correlation interactions is approximately described by generalized gradient approximation (GGA) with Perdew-Burke-Ernzerhof (PBE) functional [11]. The cut-off energy for the plane waves is 520 eV. The Monkhorst–Pack scheme [12] ***k***-point mesh is used for the integration in the first Brillouin zone, and the

* Corresponding author at: Laboratory of Computational Materials Physics, Department of Physics, Jiangxi Normal University, Nanchang 330022, China.
E-mail address: cyouyang@hotmail.com (C.Y. Ouyang).

http://dx.doi.org/10.1016/j.matlet.2016.11.013
Received 25 October 2016; Accepted 2 November 2016
Available online xxxx
0167-577X/

density of the *k*-mesh ensures that the interval of the grid is less than 0.03 $Å^{-1}$. The total potential energy is converged within 10^{-4} eV with these parameters. The Li migration pathways are optimized and the energy barriers are calculated with nudged elastic band (NEB) method [13].

3. Results and discussion

In order to model the surface characters of the Li oxides and peroxides, we first optimized the bulk atomic structures. Our results show that the theoretical lattice constants are in good agreements with the experimental data. Li_2O has cubic structure (space group: $Fm\bar{3}m$) and the optimized lattice constant is 4.635 Å, about 0.6% larger than the experimental observed 4.623 Å [14]. The Li_2O_2 structure has hexagonal lattice with the $P63/mmc$ space group. The optimized lattice constants are a=b=3.164 Å and c=7.698 Å, in very good agreement with the experimental observed a=b=3.183 Å and c=7.726 Å [15]. These results confirm that the computational method and parameters are reliable.

The surface slab models are built with the above bulk structures. To evaluate the thermodynamic stability of the surfaces, we calculated the surface energies defined as:

$$E_{surf} = (E_{slab} - E_{bulk})/2S$$

where E_{slab} and E_{bulk} represent the total energies of the slab and the bulk, respectively, S is the surface area. The low index surfaces of the Li_2O (100), (110) and (111), and Li_2O_2-(0001), (1$\bar{1}$00) and (11$\bar{2}$0) are considered. For non-stoichiometrical slab, the surface energy is obtained with reference to the energy of O_2 molecule in vacuum. The calculated surface energies are given in Table 1. As it can be seen, the Li_2O-(111) and Li_2O_2-(11$\bar{2}$0) surfaces have the lowest surface energies, in agreement with the other theoretical results [16–18]. Therefore, the Li adsorption and diffusion are considered on them. Two possible Li diffusion mechanisms are considered, namely, the Li ad-atom migration and Li vacancy migration.

Fig. 1 presents the atomic structures of the stable Li_2O-(111) and Li_2O_2-(11$\bar{2}$0) surfaces. Our results show that Li prefers to adsorb on the top sites of O atoms at the Li_2O-(111). Therefore, Li migration pathway at the Li_2O-(111) is jumping from top site to top site of O atoms, as shown by solid arrow and denoted as "Li_2O-Path-Li" in Fig. 1a. On the other hand, vacancy migration pathway is denoted as "Li_2O-Path-V" in Fig. 1a. Fig. 2 gives the energy profiles of Li migration at the Li_2O (111) surface along the optimized pathways. The energy barriers for Li ad-atom and vacancy migration are 0.45 eV and 0.98 eV, respectively. These results are substantially higher than that of Li-vacancy migration in Li_2O bulk, which is reported to range from 0.152 eV [19] to 0.26 eV [20]. Therefore, the Li diffusion at the Li_2O surface is much slower comparing with that of in the bulk, which is partly responsible for the poor rate performance of the Li-O_2 battery when the discharge product is Li_2O.

Table 1
Surface energies of different surfaces and terminations of the Li_2O and Li_2O_2.

Compounds	Surface	Surface termination	Surface energies (J/m^2)	References
Li_2O	(100)	O-terminated	2.494	2.515 [16]
		Li-terminated	6.162	6.616 [16]
		Stoichiometric	1.112	1.346 [16]
	(110)	Stoichiometric	1.101	1.025 [16] 1.240 [17]
	(111)	Stoichiometric	0.523	0.561 [16] 0.790 [17]
Li_2O_2	(1$\bar{1}$00)	Li-terminated	1.915	1.650 [18] 1.682 [16]
		Stoichiometric	0.970	0.833 [16]
	(0001)	Li-terminated	1.974	1.970 [18] 2.211 [16]
	(11$\bar{2}$0)	Stoichiometric	0.824	0.689 [18]

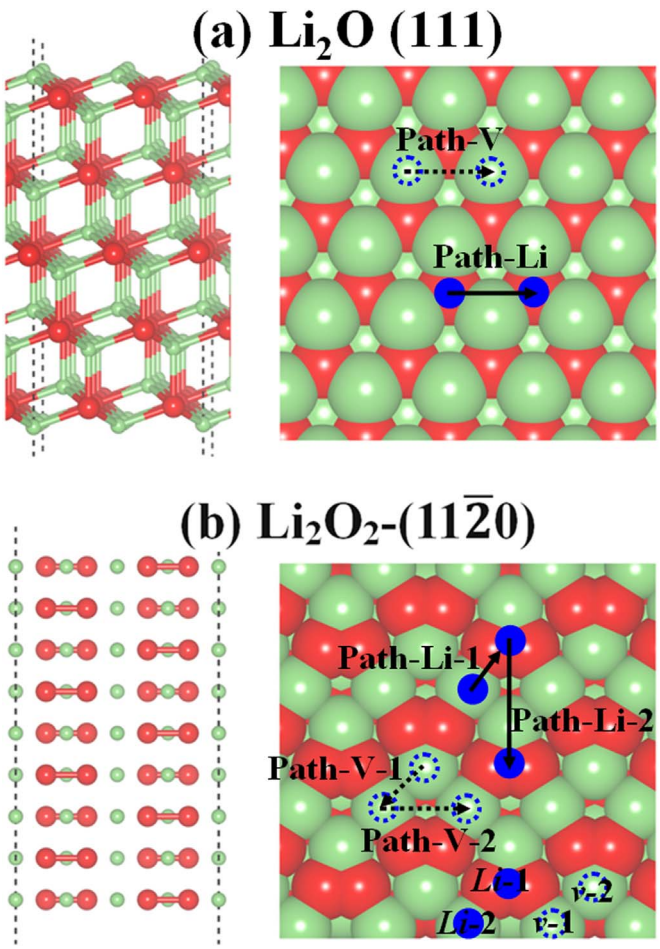

Fig. 1. The side (left) and top (right) views of the Li_2O-(111) and Li_2O_2-(11$\bar{2}$0) surfaces. The blue filled cycles are the stable Li adsorption sites, while the dashed empty cycles denote the Li vacant sites. The solid (dashed) arrows represent the migration pathways of the Li ad-atom (vacancy). (For interpretation of the references to color in this figure legend, the reader is referred to the web version of this article.)

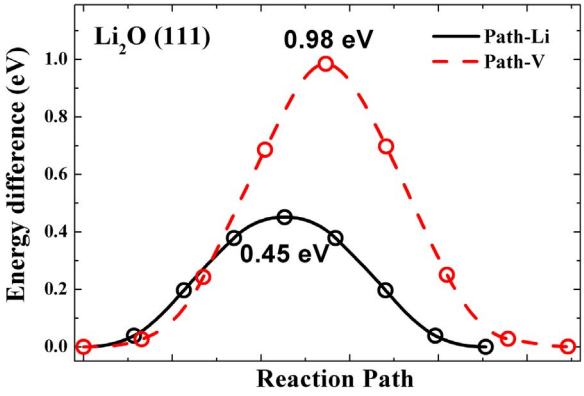

Fig. 2. Energy profiles of Li ad-atom and vacancy migration on the Li_2O (111) surface.

At the Li_2O_2 (11$\bar{2}$0) surface, there are two different Li sites and thus two different Li vacancy sites are considered and denoted as "v-1" and "v-2" in Fig. 1b. The calculated energy of v-1 is about 0.43 eV lower than v-2. Two independent vacancy migration pathways are considered, namely, migration from v-2 to v-1 (denoted as "Path-V-1" in Fig. 1b) and migration from v-1 to v-1 (denoted as "Path-V-2" in Fig. 1b). The energy profiles for the Li vacancy migration along the above two pathways are given in Fig. 3a. The vacancy moves from the